Interaction of adsorbates with electric-field fluctuations near surfaces: Nonradiative lifetimes and energy-level shifts

D. L. Mills, J. X. Cao, and Ruqian Wu
Department of Physics and Astronomy, University of California, Irvine, California 92697, USA
(Received 2 February 2007; published 29 May 2007)

In the vacuum above surfaces, there are zero-point fluctuations in the electromagnetic field generated by zero-point charge fluctuations in the substrate. A molecule near the surface will couple to such fluctuations, with the consequence that excited states may decay via nonradiative transitions in which energy is transferred to the electronic excitations of the substrate (surface plasmons, particle hole pairs). In addition, coupling to the fluctuations will produce energy-level shifts not included in the standard version of density-functional theory. We develop a formalism that allows one to calculate the nonradiative lifetimes from this interaction, and also the energy-level shifts. We treat the electric-field fluctuations within the framework of a phenomenological theory that relates their amplitude and frequency spectrum to the optical dielectric constants of the materials from which the substrate complex is fabricated. We demonstrate that when the formalism is applied to a structureless, highly localized electron, the energy-level shift is just that given by the image potential of classical dielectric theory. In real systems one must include the effect of virtual transitions to excited states in the analysis of the level shifts. We present a quantitative study of the nonradiative lifetime of the lowest unoccupied molecular orbital (LUMO)+1 state of the magnesium porphine molecule, adsorbed on the oxide covered NiAl(110) surface, along with calculations of the energy-level shifts induced by the field fluctuations for this system. Our calculated nonradiative lifetime is in good accord with experimental data.

DOI: 10.1103/PhysRevB.75.205439 PACS number(s): 78.67.−n, 78.68.+m

I. INTRODUCTION

It is the case in recent years that the scanning tunneling microscope (STM) has emerged as a most powerful spectroscopic tool. By now the technique has been used to study the vibrational normal modes of single molecules[1] or atoms,[2] and it is also used to study electronic energy levels of diverse isolated, single adsorbate atoms or molecules, including the vibronic sidebands.[3] However, it is often difficult, indeed impossible, to study details of electronic structure, including vibronic sidebands, if the molecule of interest is chemisorbed directly on the metallic substrate into which the electrons from the STM tip tunnel. The reason is that the molecular energy levels are broadened dramatically, by virtue of hybridization between the molecular orbitals and the electronic states of the substrate. In the latter, there will be a continuum of final states, so the molecular level is broadened into a virtual level whose width may be several tenths of an electron volt. Thus much detail is obscured in the spectroscopy of such entities.

As a consequence, it is most useful to employ a metallic substrate covered by a few Å of insulating oxide. If the oxide layer is not too thick, electrons from the STM tip may still tunnel through the oxide barrier, thus rendering STM based single molecule spectroscopy viable. At least to first approximation, one may ignore direct hybridization between the molecular orbitals and the electron states of the metallic substrate under the oxide layer. The excited states of the molecule are thus quite sharp in energy, hence allowing fine details of the electronic and vibrational structures to be resolved in STM based spectroscopy. The oxidized NiAl(110) surface has emerged as an important oxide layer and substrate combination. A very lovely example of this form of STM based spectroscopy is found in Ref. 4.

Even though one may ignore the effects of direct hybridization between the molecule and the electrons in the metallic substrate in the circumstances described in the previous paragraph, it is the case that the molecule may couple to the electronic degrees of freedom in the substrate. Electrons within the substrate necessarily undergo thermodynamic fluctuations in charge density. Even at zero temperature, there are zero-point fluctuations present. These charge fluctuations produce fluctuating electric fields in the vacuum just above the surface, by virtue of the long-ranged character of the Coulomb interaction. Electrons inside a molecule on the oxide layer will interact with the electrons in the substrate through these electric-field fluctuations, even though no direct hybridization is present. Through this mechanism, the continuum of particle-hole fluctuations in the substrate, along with collective excitations such as surface plasmons of the oxide-substrate complex, will influence the adsorbate. As we shall see below, this interaction has two effects. Excited states of the molecule acquire a finite lifetime by virtue of nonradiative transitions to lower-lying unoccupied levels, and in addition there are shifts in the energy levels of the adsorbate.

It is the purpose of this paper to develop the theory of interactions of molecules or other entities near substrates with the fluctuations in electric field just described. After the formalism is developed, we present explicit calculations for the nonradiative lifetime of excited states of the magnesium porphine molecule adsorbed on the oxide covered NiAl(110) surface. This is the system studied in Ref. 4, and our results are in good agreement with the measured width of the lowest unoccupied molecular orbital (LUMO)+1 state of this species. Some general remarks are in order before we proceed.

Our approach to the description of the electric-field fluctuations above the substrate is closely related to an elegant

discussion given some years ago of the nature of electromagnetic fluctuations near solid materials, along with their consequences.[5] These authors begin by analyzing the structure of the full quantum field-theoretic Green's functions for the electromagnetic fields in and near materials. They point out that if one may, within the framework of the full quantum theory, define a dielectric response function for the material system, then the retarded Green's functions of the quantum theory of the electromagnetic field obey precisely the same differential equations and boundary conditions as the Green's functions of classical electromagnetic theory. Thus one may express the spectral densities of the field-theoretic propagators in terms of the Green's functions of the classical Maxwell equations. If the complex dielectric function measured optically is employed in this theoretical structure, then one obtains a rigorous account of those field fluctuations whose length scale is long compared to a lattice constant. Within this framework, one may analyze electric-field fluctuations and their influence near real materials and material combinations by utilizing measured data for the optical response characteristic of the constituent materials.

This approach was used by one of the present authors many years ago, to construct a general theory of the dipole losses experienced by low-energy electrons as they reflect off surfaces.[6] Such dipole losses may be viewed as having their origin in the inelastic scattering of electrons in the beam from the electric-field fluctuations in the vacuum above the crystal produced by the diverse elementary excitations probed by this form of spectroscopy. This approach to the theory led to very good accounts of electron energy-loss spectra,[7] including losses from structures whose length scale extends down to microscopic lengths.[8,9] By adopting this approach to address the issues of current interest to us, we put forth in this paper a formalism which allows calculations to be carried out readily for a given adsorbate on diverse substrates, with knowledge of only the optical response of the latter.

In addition to calculating the contribution to the nonradiative lifetime of excited states, we address a second issue in the theoretical structure set forth here. Density-functional theory is, of course, used very widely in the analysis of adsorbates on surfaces and by this time the approach enjoys very impressive success. However, when applied to surfaces, in this method (in its standard form), the surface potential experienced by the adsorbate falls off exponentially as one moves into the vacuum from the substrate. It is the case, in fact, that an electron near any solid surface experiences an image potential whose origin is in the long-ranged Coulomb interaction. Surely the image potential will produce shifts in energy levels of adsorbed species such as we consider in the present paper. Such level shifts are not incorporated in standard density-functional descriptions, and one must then inquire into their magnitude and thus the accuracy of density-functional theory when applied to adsorbates. In our formalism, the electric-field fluctuations outside the surface lead to not only nonradiative decay of excited states but also energy-level shifts of all states, as mentioned above. When we apply our formalism to a highly localized "sterile electron," which resides in a single orbital with no excited states, our expression for the energy-level shift reduces exactly to the shift in energy of the electron produced by the image potential. A real system, of course, has a spectrum of excited states and the electric-field fluctuations produce virtual transitions to these states, which we shall see also contribute to the energy shift. Thus one cannot modify density-functional theory to include image potential effects by simply introducing an effective image potential from electrostatic theory. One should use the term dynamical image potential shift when referring to this phenomenon, since virtual fluctuations enter in addition to the shift produced by the static, classical image potential. The calculations reported below explore these effects through numerical calculations, for the particular system studied experimentally in Ref. 4.

We should note that it is possible to incorporate long-ranged forces (image potentials, van der Waals forces) into density-functional theory.[10] However, to date the applications are to systems considerably simpler than that explored here and envisioned for our future work, and it is the case as well that only rather few studies have appeared in the literature. As we shall see below, for suitable systems our approach allows one to extend standard density-functional calculations to include such effects on both ground state and excited states, through use of optical data on the substrate and other constituents.

In this paper, our attention is confined to an adsorbate which is near a metal surface, possibly covered by an oxide layer. In the experiments reported in Ref. 4, of course, the STM tip is very close to the adsorbed molecule as well. Its presence will affect the nature of the electric-field fluctuations in the vicinity of the adsorbate. Using the mathematical description we have developed of the influence of STM tips on nonlinear optical probes of molecules near and under the tip,[11] it is a straightforward matter in principle to extend the analysis here to incorporate the role of the nearby STM probe. This issue is under study at present.

The outline of this paper is as follows. In Sec. II, we develop the formalism and discuss aspects of the results in general terms. In Sec. III, we present density-functional studies of the uncharged and charged magnesium porphine molecule in free space, and compare the results with the data reported in Ref. 4. We then discuss our studies of the lifetime of the LUMO+1 level produced by coupling to the electric-field fluctuations from the substrate, and we also discuss our calculations of the dynamic image potential induced shifts of the energy levels of the molecule. Section IV is devoted to final remarks and comments on the implications of our remarks.

II. FORMALISM

A. General development

As discussed in Sec. I, we have in mind the following geometry. One has a substrate, possibly metallic, on which an oxide layer is grown. On top of the oxide layer, we have an adsorbate atom or possibly a more complex molecule. We shall describe electrons within the molecule by introducing the appropriate many-body Green's function. Our aim is then to derive an expression for the contribution to the proper self-energy associated with the Green's function, along with

the Dyson's equation it obeys, where the origin of the proper self-energy lies in the interaction of electrons within the molecule with the electric-field fluctuations discussed in Sec. I. We should remark that the derivation below applies only to the case where the temperature T is taken to be zero. This will be quite fine for the applications we envision, where the energy scale of interest is eV. Thus when we consider the influence of electric-field fluctuations of frequency ω, we shall always be in the regime where $\hbar\omega \gg k_B T$. It is the case, however, that our description of the spectral character of the electrostatic field fluctuations near the surface is carried out for finite temperatures. This will allow us to extend our formalism to finite temperatures in the future, if desired, and the resulting expressions may be useful for other applications.

We wish the oxide layer to be thick enough that to good approximation the adsorbate is described by a set of wave functions $\{\varphi_\alpha(\vec{r})\}$ which may be viewed as distinct from the electrons in the metallic substrate and oxide layer. We assume these wave functions and the associated energies $\{\varepsilon_\alpha\}$ are generated through use of an appropriate density-functional calculation. We shall use H_a to describe the Hamiltonian from which the adsorbate eigenfunctions and eigenvalues are generated. In the metal substrate and also the oxide layer, we have electrons described by a set of eigenfunctions $\{\psi_m(\vec{r})\}$. In future applications we envision that an STM tip will be located just above the adsorbate. In this case, the set of eigenfunctions and eigenvalues associated with the metallic structure will include those within the STM tip as well. These various states and energy levels are described by a Hamiltonian we call H_M. We begin by thinking of two distinct systems of electrons described by a fermion field operator which takes the form, in the Schrödinger representation,

$$\psi(\vec{r}) = \psi_a(\vec{r}) + \psi_M(\vec{r}), \tag{1}$$

where we may write $\psi_a(\vec{r}) = \Sigma_\alpha c_\alpha \varphi_\alpha(\vec{r})$ and $\psi_M(\vec{r}) = \Sigma_m c_m \psi_m(\vec{r})$, with c_α and c_m the relevant fermion annihilation operators. The Hamiltonian of these two sets of electrons is then

$$H_0 = H_a + H_M, \tag{2}$$

where we shall not need explicit forms for H_a and H_M in what follows.

The electrons in the adsorbate interact with those in the substrate through the long-ranged Coulomb interaction, which has the form

$$V = e\int d^3 r \psi_a^+(\vec{r})\Phi(\vec{r})\psi_a(\vec{r}), \tag{3}$$

where

$$\Phi(\vec{r}) = e\int_V d^3 r' \frac{\psi_M^+(\vec{r}')\psi_M(\vec{r}')}{|\vec{r}-\vec{r}'|}. \tag{4}$$

The integration in Eq. (4) extends over the substrate-oxide complex, and the STM tip as well, if we wish to incorporate its influence. The total Hamiltonian of our system is then

$$H = H_a + H_M + V. \tag{5}$$

We shall study the Green's function of the adsorbate complex, which is defined to be

$$G_a(\vec{r},t;\vec{r}',t') = -i\langle T(\psi_a(\vec{r},t)\psi_a^+(\vec{r}',t'))\rangle, \tag{6}$$

where $\psi_a(\vec{r},t) = \exp(iHt)\psi_a(\vec{r})\exp(-iHt)$ is the adsorbate electron Green's function in the Heisenberg representation. Our convention is that when the time arguments are omitted from operators, it is understood that they are in the Schrödinger representation, and when a time argument is present, the operator is in the Heisenberg representation. In this section, we shall employ units where $\hbar = 1$ to keep the expressions simple. The factors of $\hbar$ will be restored in the final expressions.

Through standard methods of many-body theory, it is possible to derive a Dyson equation, which is satisfied by the adsorbated Green's function. This has the form

$$\left(i\frac{\partial}{\partial t} - H_a\right)G_a(\vec{r},t;\vec{r}',t') - \int d^3 r'' dt'' \Sigma(\vec{r},t;\vec{r}'',t'')G_a(\vec{r}'',t'';\vec{r}',t') = \delta(\vec{r}-r')\delta(t-t'). \tag{7}$$

To lowest order in the electrostatic potential fluctuations, the proper self-energy in Eq. (7) is given by

$$\Sigma(\vec{r},t;\vec{r}',t') = -e^2 G_a^{(0)}(\vec{r},t;\vec{r}',t')\langle T(\Phi(\vec{r}',t')\Phi(\vec{r},t))\rangle, \tag{8}$$

where $G_a^{(0)}(\vec{r},t;\vec{r}',t')$ is the adsorbate Green's function, calculated in the limit where the Coulomb interaction V is set to zero. We next Fourier transform all quantities with respect to time:

$$G_a(\vec{r},t;\vec{r}',t') = \int \frac{d\varepsilon}{2\pi} G_a(\vec{r},\vec{r}';\varepsilon)\exp[-i\varepsilon(t-t')] \tag{9}$$

and

$$\langle T(\Phi(\vec{r},t)\Phi(\vec{r}',t'))\rangle = \int \frac{d\Omega}{2\pi}\Pi(\vec{r},\vec{r}';\Omega)\exp[-i\Omega(t-t')]. \tag{10}$$

Then Dyson's equation assumes the form

$$(\varepsilon - H_a)G_a(\vec{r},\vec{r}';\varepsilon) - \int d^3 r'' \Sigma(\vec{r},\vec{r}'';\varepsilon)G_a(\vec{r}'',r';\varepsilon) = \delta(\vec{r}-\vec{r}'), \tag{11}$$

where we have

$$\Sigma(\vec{r},\vec{r}';\varepsilon) = -e^2\int_{-\infty}^{+\infty}\frac{d\Omega}{2\pi}G_a^{(0)}(\vec{r},\vec{r}';\varepsilon+\Omega)\Pi(\vec{r}',\vec{r};\Omega). \tag{12}$$

In what follows, it will be important to note the limits in the integrations over internal frequency Ω which appear in the various statements. It is an elementary matter to calculate the adsorbate Green's function which enters Eq. (12):

$$G_a^{(0)}(\vec{r},\vec{r}';\varepsilon) = \sum_\alpha \varphi_\alpha(\vec{r})\varphi_a(\vec{r}')^* \left\{ \frac{(1-f_\alpha)}{\varepsilon - \varepsilon_\alpha + i\eta} + \frac{f_\alpha}{\varepsilon - \varepsilon_\alpha - i\eta} \right\}. \tag{13}$$

In Eq. (13), the energies ε_α are those which emerge from the solution of the Kohn-Sham equation, and the orbitals $\{\varphi_\alpha(\vec{r})\}$ are those which emerge from the same equation while f_α is unity if state α is occupied, and zero if it is not. The energies ε_α are measured from the Fermi level.

The heart of our discussion is the means we use to describe the spectral density $\Pi(\vec{r}',\vec{r};\Omega)$ associated with the fluctuations in electrostatic potential in the vicinity of the adsorbed molecule. In the next portion of our discussion, as we derive the form of $\Pi(\vec{r}',\vec{r};\Omega)$, we shall assume that the temperature T is finite. As remarked in Sec. I, it will be useful for other purposes to have the full finite temperature description of the potential fluctuation spectrum. To remind the reader that this is so, we use the notation $\langle T(\Phi(\vec{r},t)\Phi(\vec{r}',t'))\rangle_T$ to describe the finite temperature electrostatic potential propagator.

Rather than deal with the time-ordered propagator mentioned in the previous paragraph, we will study the simple correlation function $\langle\Phi(\vec{r},t)\Phi(\vec{r}',t')\rangle_T$, where we notice the time-ordering operator is missing in this function. We write

$$\langle\Phi(\vec{r},t)\Phi(\vec{r}',t')\rangle_T = \int_{-\infty}^{+\infty} \frac{d\Omega}{2\pi} P(\vec{r},\vec{r}';\Omega)\exp[-i\Omega(t-t')]. \tag{14}$$

It is a short exercise in Fourier analysis to obtain the relationship

$$\Pi(\vec{r},\vec{r}';\Omega) = \int_{-\infty}^{+\infty} \frac{d\omega}{2\pi i}\left(\frac{P(\vec{r}',\vec{r};\omega)}{(\Omega+\omega-i\eta)} - \frac{P(\vec{r},\vec{r}';\omega)}{(\Omega-\omega+i\eta)} \right). \tag{15}$$

We may now insert Eqs. (13) and (15) into Eq. (12), and carry out the integration over Ω. The proper self-energy may then be cast into the form

$$\Sigma(\vec{r},\vec{r}';\varepsilon) = -\frac{e^2}{2\pi}\sum_\alpha \varphi_\alpha(\vec{r})\varphi_\alpha(\vec{r}')^* \times\left(\int_{-\infty}^{+\infty} \frac{d\omega(1-f_\alpha)P(\vec{r}',\vec{r};\omega)}{(\varepsilon-\varepsilon_\alpha-\omega+i\eta)} + \int_{-\infty}^{+\infty} \frac{d\omega f_\alpha P(\vec{r},\vec{r}';\omega)}{(\varepsilon-\varepsilon_\alpha+\omega-i\eta)} \right). \tag{16}$$

To obtain an expression for $P(\vec{r},\vec{r}';\omega)$ which appears in Eq. (16), we proceed as follows. We introduce yet another form of the electrostatic potential propagator:

$$D_{\Phi\Phi}(\vec{r},t;\vec{r}',t') = i\theta(t-t')\langle[\Phi(\vec{r},t),\Phi(\vec{r}',t')]\rangle_T. \tag{17}$$

If we define

$$\rho_{\Phi\Phi}(\vec{r},\vec{r}';\omega) = i\{D_{\Phi\Phi}(\vec{r},\vec{r}';\omega+i\eta) - D_{\Phi\Phi}(\vec{r}',\vec{r};\omega+i\eta)^*\}, \tag{18}$$

then one may establish the relationship

$$P(\vec{r},\vec{r}';\omega) = [1+n(\omega)]\rho_{\Phi\Phi}(\vec{r},\vec{r}';\omega), \tag{19}$$

where $n(\omega)=1/[\exp(\beta\omega)-1]$ is the Bose Einstein function.

The reason for the above manipulations now follows. The function $D_{\Phi\Phi}(\vec{r},\vec{r}';\omega+i\eta)$ is a response function with the following physical meaning. Suppose we place some external charge in the near vicinity of our substrate complex (with adsorbate absent). Let the external charge density have the form $\rho_{ext}(\vec{r};\omega)\exp[-i(\omega+i\eta)t]$. Then from linear-response theory, one may show that the expectation value of the electrostatic potential operator $\langle\Phi(\vec{r},t)\rangle_T$ is given by

$$\langle\Phi(\vec{r},t)\rangle_T = \exp[-i(\omega+i\eta)t] \times \int d^3r' D_{\Phi\Phi}(\vec{r},\vec{r}';\omega+i\eta)\rho_{ext}(\vec{r}';\omega). \tag{20}$$

Our remaining task is to construct the response function which appears on the right-hand side of Eq. (20). Here we resort to the elegant arguments presented in Ref. 3. In principle, we should study the structure in Eq. (17), where the right-hand side involves the stated commutator of the Heisenberg operators associated with the electrostatic potential. The authors of Ref. 3 point out that if the response of the media to external charge can be described in terms of a possibly spatially varying, complex dielectric constant $\varepsilon(\vec{r},\omega+i\eta)$, then the differential equation obeyed by the full quantum theoretical response function introduced in Eq. (17) is precisely the same as that obeyed by the Green's function of classical electromagnetic theory. In a complete theory, of course, to calculate the dielectric response function one must resort to a full quantum theory. However, if one expresses the response function in Eq. (17) in terms of the appropriate dielectric constants, and if one then obtains the dielectric functions needed from experimental data, then one has a full and rigorous account of the response of the system, and also of the electromagnetic fluctuations in and around it. The latter follows when one uses the prescriptions we have given above for the construction of the spectral density function defined in Eq. (14). In the numerical calculations reported in Sec. II, we employ optically measured dielectric constants to obtain a description of the electromagnetic fluctuations in the spectral regions of interest to the present analysis. By this procedure, we obtain a fully rigorous account, for real materials, of potential fluctuations whose length scale is long compared to microscopic lengths, such as lattice constants. We shall appreciate that for the large molecule of interest to us, length scales large compared to a lattice constant provide the dominant contribution to the self-energy.

Now in the applications we envision here, we will be dealing with structures whose length scale is small compared to the wavelength of electromagnetic radiation in the frequency domain of interest. We shall suppose we are interested in frequencies in the optical frequency domain, and the structures we explore have length scales of only a nanometer

or so. Hence we shall use electrostatic theory to describe the response of the system. We thus calculate the Green's function by solving

$$\vec{\nabla}\cdot[\varepsilon(\vec{r},\omega+i\eta)\vec{\nabla}D_{\Phi\Phi}(\vec{r},\vec{r}';\omega+i\eta)]=-4\pi\delta(\vec{r}-\vec{r}'). \tag{21}$$

For the case of a substrate with dielectric constant $\varepsilon_{sub}(\omega)$ covered by a film of thickness d whose dielectric constant is $\varepsilon_{ox}(\omega)$, one may work out the form of the spectral density function defined in Eq. (18). One finds

$$\rho_{\Phi\Phi}(\vec{r},\vec{r}';\omega)=\frac{2}{\pi}\int\frac{d^2Q_\parallel}{Q_\parallel}\exp[i\vec{Q}_\parallel\cdot(\vec{r}_\parallel-\vec{r}'_\parallel)]\times\exp[-Q_\parallel(z+z')]\mathrm{Im}\left\{\frac{-1}{1+\tilde{\varepsilon}(Q_\parallel,\omega)}\right\}, \tag{22a}$$

where

$$\tilde{\varepsilon}(Q_\parallel,\omega)=\varepsilon_{ox}(\omega)\left(\frac{1+\Delta(\omega)\exp(-2Q_\parallel d)}{1-\Delta(\omega)\exp(-2Q_\parallel d)}\right) \tag{22b}$$

with

$$\Delta(\omega)=[\varepsilon_{sub}(\omega)-\varepsilon_{ox}(\omega)]/[\varepsilon_{sub}(\omega)+\varepsilon_{ox}(\omega)]. \tag{22c}$$

It should be noted that we assume the outer surface of the oxide layer is located in the xy plane, where $z=0$.

We have one final point to consider. The treatment given of the fluctuations in the electrostatic potential applies to finite temperatures, whereas the derivation of the expression for the proper self-energy made explicit use of the fact that the temperature was zero. Hence we need to insert the expression for the spectral density function in Eq. (16) appropriate to zero temperature. As the temperature T is taken to zero, for positive frequencies $1+n(\omega)\to 1$, while for negative frequencies, $1+n(\omega)\to 0$. Hence for the proper self-energy we have the final form

$$\Sigma(\vec{r},\vec{r}';\varepsilon)=-\frac{e^2}{2\pi}\sum_\alpha\varphi_\alpha(\vec{r})\varphi_\alpha(\vec{r}')^*\times\left(\int_0^\infty d\omega\frac{(1-f_\alpha)\rho_{\Phi\Phi}(\vec{r}',\vec{r};\omega)}{(\varepsilon-\varepsilon_\alpha-\omega+i\eta)}+\int_0^\infty d\omega\frac{f_\alpha\rho_{\Phi\Phi}(\vec{r},\vec{r}';\omega)}{(\varepsilon-\varepsilon_\alpha+\omega-i\eta)}\right). \tag{23}$$

We now have the Dyson equation in hand, and the proper self-energy describes both energy-level shifts and also lifetimes produced by nonradiative decay to the electronic excitations in the substrate. The latter follow from the imaginary part of the proper self-energy. In the next section we discuss the means of solving the Dyson equation, for the system of interest.

B. A perturbation theoretic solution of Dyson's equation

We begin by expressing the proper self-energy in the form

$$\Sigma(\vec{r},\vec{r}';\varepsilon)=-\sum_\alpha\varphi_\alpha(\vec{r})S_\alpha(\vec{r},\vec{r}';\varepsilon)\varphi_\alpha(\vec{r}')^*, \tag{24}$$

where

$$S_\alpha(\vec{r},\vec{r}';\varepsilon)=\frac{e^2}{2\pi}\int_0^\infty d\omega\rho_{\Phi\Phi}(\vec{r},\vec{r}';\omega)\left(\frac{(1-f_\alpha)}{(\varepsilon-\varepsilon_\alpha-\omega+i\eta)}+\frac{f_\alpha}{(\varepsilon-\varepsilon_\alpha+\omega-i\eta)}\right). \tag{25}$$

Notice, by the way, that the spectral density of the electrostatic potential fluctuations is unchanged when $\vec{r}$ and $\vec{r}'$ are interchanged.

We next assume the functions $\{\varphi_\alpha(\vec{r})\}$ form a complete, orthonormal set so that we can write

$$\delta(\vec{r}-\vec{r}')=\sum_\beta\varphi_\beta(\vec{r})\varphi_\beta(\vec{r}')^* \tag{26}$$

and then we can seek a representation of the adsorbate Green's function in the form

$$G_a(\vec{r},\vec{r}';\varepsilon)=\sum_{\alpha,\alpha'}\varphi_\alpha(\vec{r})\varphi_{\alpha'}(\vec{r}')^*g_{\alpha\alpha'}(\varepsilon). \tag{27}$$

Then Dyson's equation becomes

$$(\varepsilon-\varepsilon_\alpha)g_{\alpha,\alpha'}(\varepsilon)+\sum_\gamma\Sigma_{\alpha,\gamma}(\varepsilon)g_{\gamma,\alpha'}(\varepsilon)=\delta_{\alpha,\alpha'}, \tag{28}$$

where

$$\Sigma_{\alpha,\gamma}(\varepsilon)=\sum_\beta\int d^3rd^3r'\varphi_\alpha(\vec{r})^*\varphi_\beta(\vec{r})S_\beta(\vec{r},\vec{r}';\varepsilon)\varphi_\beta(\vec{r}')^*\varphi_\gamma(\vec{r}'). \tag{29}$$

From the structure of Eq. (28), one sees that the potential fluctuations in which the adsorbate is embedded provide a cross coupling between the states that are viewed as independent eigenstates within the framework of density-functional study theory.

Our interest is in the first correction to density-functional theory. To lowest order, $g_{\alpha,\alpha'}(\varepsilon)$ remains diagonal, and we may write

$$\Sigma_{\alpha,\alpha}(\varepsilon_\alpha)=\frac{e^2}{\pi^2}\int_0^\infty d\omega\int\frac{d^2Q_\parallel}{Q_\parallel}\mathrm{Im}\left\{\frac{-1}{1+\tilde{\varepsilon}(Q_\parallel,\omega)}\right\}\times\sum_\beta|\langle\alpha|\exp[i\vec{Q}_\parallel\cdot\vec{r}_\parallel-Q_\parallel z\ |\beta\rangle|^2\times\left\{\frac{f_\beta}{(\varepsilon_\alpha-\varepsilon_\beta+\omega-i\eta)}+\frac{(1-f_\beta)}{(\varepsilon_\alpha-\varepsilon_\beta-\omega+i\eta)}\right\}. \tag{30}$$

In the sum over states in Eq. (30), one should retain the diagonal term with $\beta=\alpha$. This particular term can be arranged in a more convenient form. For the moment, we denote it by $\Sigma^{(D)}_{\alpha,\alpha}$, and upon setting $\varepsilon_\beta=\varepsilon_\alpha$ we have

$$\Sigma^{(D)}_{\alpha,\alpha} = \frac{e^2}{\pi^2}(2f_\alpha - 1)\int \frac{d^2Q_\parallel}{Q_\parallel}|\langle\alpha|\exp(i\vec{Q}_\parallel\cdot\vec{r}_\parallel - Q_\parallel z)|\alpha\rangle|^2 \times \int_0^\infty \frac{d\omega}{\omega}\,\mathrm{Im}\left\{\frac{-1}{1+\tilde{\varepsilon}(Q_\parallel,\omega)}\right\}. \quad (31)$$

If the state α is occupied, then of course f_α is unity, and it is zero if the state is unoccupied. Thus the self-energy correction in Eq. (31) has the opposite sign for occupied and unoccupied states. Recall that the pole of the single-particle Green's function occurs at the excitation energies of the system. If the state α is occupied, we have in Eq. (31) a contribution to the excitation energy of an electron state. If the state is unoccupied, it is the excitation energy of a hole state that is described. We shall appreciate shortly that, in essence, the real part of the self-energy describes an energy shift which is, in essence, the image potential shift. The contributions of the image potential to the excitation energy of an electron and a hole have opposite signs.

Now the response function $\tilde{\varepsilon}(Q_\parallel,\omega)$, considered as a function of frequency in the complex ω plane for fixed $Q_\parallel$, has analytic properties identical to that of an optical dielectric constant $\varepsilon(\omega)$. For the latter, one has the sum rule[12]

$$\frac{\varepsilon(ix)-1}{\varepsilon(ix)+1} = \frac{4}{\pi}\int_0^\infty \frac{d\omega\omega}{\omega^2+x^2}\,\mathrm{Im}\left\{\frac{-1}{1+\varepsilon(\omega)}\right\}. \quad (32)$$

We may use this for $x=0$ to evaluate the frequency integral in Eq. (31). We then have

$$\Sigma^{(D)}_{\alpha,\alpha} = \frac{e^2}{4\pi}(2f_\alpha - 1)\int \frac{d^2Q_\parallel}{Q_\parallel}|\langle\alpha|\exp(i\vec{Q}_\parallel\cdot\vec{r}_\parallel - Q_\parallel z)|\alpha\rangle|^2 \times \left\{\frac{\tilde{\varepsilon}(Q_\parallel,0)-1}{\tilde{\varepsilon}(Q_\parallel,0)+1}\right\}. \quad (33)$$

Our final expression for the proper self-energy can thus be written in the form

$$\Sigma_{\alpha,\alpha} = \Sigma^{(D)}_{\alpha,\alpha} + \delta\Sigma_{\alpha,\alpha}, \quad (34a)$$

$$\delta\Sigma_{\alpha,\alpha} = +\frac{e^2}{\pi^2}\int_0^\infty d\omega \int \frac{d^2Q_\parallel}{Q_\parallel}\,\mathrm{Im}\left\{\frac{-1}{1+\tilde{\varepsilon}(Q_\parallel,\omega)}\right\} \times \sum_{\beta\neq\alpha}|\langle\alpha|\exp(i\vec{Q}_\parallel\cdot\vec{r}_\parallel - Q_\parallel z)|\beta\rangle|^2 \times \left\{\frac{f_\beta}{(\varepsilon_\alpha-\varepsilon_\beta+\omega-i\eta)} + \frac{(1-f_\beta)}{(\varepsilon_\alpha-\varepsilon_\beta-\omega+i\eta)}\right\}. \quad (34b)$$

The first term on the right-hand side of Eq. (34a), $\Sigma^{(D)}_{\alpha,\alpha}$ is, of course purely real. The second term contains both a real and an imaginary part. The real part is the contribution to the energy shift of state α from fluctuation induced virtual transitions to other states, and the imaginary part of the second term describes the nonradiative lifetime due to the transfer of energy to the excitations in the substrate via the long-ranged part of the Coulomb interaction. This is the nonradiative lifetime of the excited level.

We end this section by evaluating Eq. (34a) for a highly localized "sterile" electron located a distance z_0 above a substrate whose dielectric constant is $\varepsilon_{sub}(\omega)$. The term "sterile" refers to an electron with no excited state; it sits frozen in state α. Then $\delta\Sigma_{\alpha,\alpha}$ vanishes, and the only contribution to the proper self-energy comes from $\Sigma^{(D)}_{\alpha,\alpha}$. We omit the oxide layer by setting its dielectric constant to unity. If the state α is highly localized around a point located the distance z_0 above the substrate, then we have

$$|\langle\alpha|\exp(i\vec{Q}_\parallel\cdot\vec{r}_\parallel - Q_\parallel z)|\alpha\rangle|^2 = \exp(-2Q_\parallel z_0). \quad (35)$$

Thus for such an electron we have, assuming the state is occupied,

$$\Sigma^{(D)}_{\alpha,\alpha} = \frac{e^2}{4\pi}\left\{\frac{\varepsilon_{sub}(0)-1}{\varepsilon_{sub}(0)+1}\right\}\int \frac{d^2Q_\parallel}{Q_\parallel}\exp(-2Q_\parallel z_0). \quad (36)$$

The integral in Eq. (36) is elementary, and we have

$$\Sigma^{(D)}_{\alpha,\alpha} = \frac{e^2}{4z_0}\left\{\frac{\varepsilon_{sub}(0)-1}{\varepsilon_{sub}(0)+1}\right\}. \quad (37)$$

This is exactly the energy shift experienced by an electron placed near a dielectric surface, by virtue of the classical image potential (this shift is the work required to bring the electron from infinity, to the distance z_0 from the surface).

Thus the energy-level shift produced by the lowest-order self-energy correction associated with the interaction of the electron with electric-field fluctuations above the surface is, for the sterile electron, just the image potential energy from classical dielectric theory. A real adsorbate, of course, has a whole spectrum of energy levels, and in this circumstance to evaluate the energy shift it is essential to take due account of fluctuation induced virtual transitions to excited states, as described by the second term on the right-hand side of Eq. (34). It is incorrect to use a simple static electrostatic potential to describe corrections to density-functional theory from the long-ranged tail of the Coulomb interaction between the electrons in the adsorbate, and those in a nearby substrate.

This completes our discussion of the formalism we have developed. In the next section we describe the numerical calculations we have carried out with it.

III. NUMERICAL CALCULATIONS

A. Free-standing magnesium porphine molecule

In this section, we shall describe our density-functional studies of the free-standing magnesium porphine molecule. We shall see that we can obtain quite a good account of the data reported in Ref. 4 for the energy levels of this molecule in both its charged and uncharged states, when it is adsorbed on the oxide covered NiAl(110) surface. This reinforces the notion that when we discuss the lifetime of excited states, to good approximation our assumption that overlap between the orbitals associated with the adsorbate and those associated with the substrate electron can be set aside.

The calculations for the free Mg-porphine molecule are conducted with the plane-wave and pseudopotential based VASP code as well as the all-electron DMol method,[13] at the

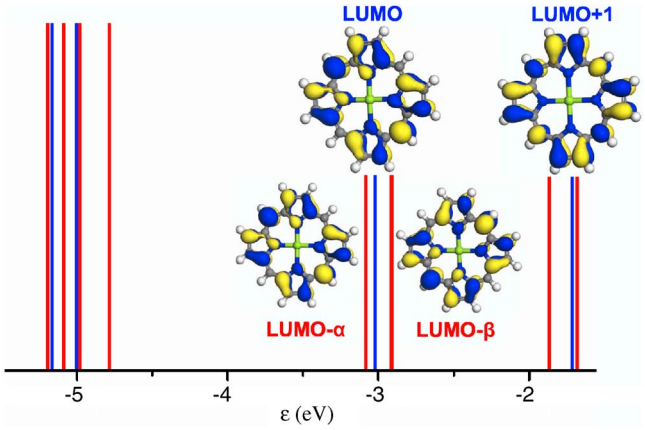

FIG. 1. (Color online) The calculated energy levels and wave functions for neutral (in blue/dark gray) and $-e$ charged (in red/light gray) free-standing Mg-porphine molecules.

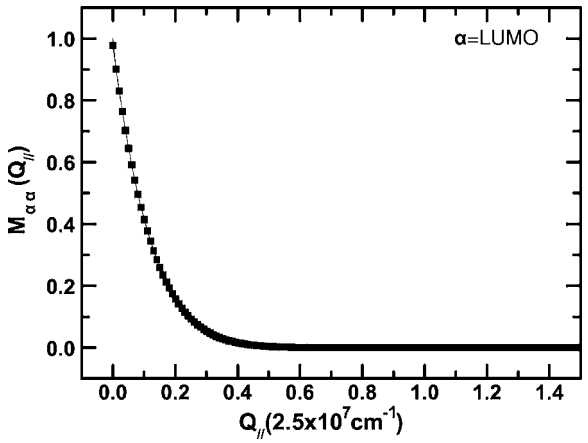

FIG. 2. The quantity $M_{\alpha\alpha}(\vec{Q}_{\parallel})$, defined in the text, is plotted as a function of the LUMO orbital. Here the wave vector $\vec{Q}_{\parallel}$ is directed along the (100) direction.

level of generalized gradient approximation. The revised Perdew-Burke-Enzerhof[14] functional was adopted for the description of exchange-correlation interaction among electrons. In DMol calculations, we used the double-numeric quality bases with polarization functions and the global orbital cutoff was set to be 5.0 Å. In the VASP calculations, a supercell of 25 Å in each dimension is used to mimic the single Mg-porphine molecule. This unit cell is sufficiently large that near its periphery, the amplitude of all the states is very small. The atomic structures are optimized through total-energy minimization procedures guided by the calculated atomic forces.

Calculations with both approaches give basically the same results, indicating that the all-electron treatment is insignificant for the neutral Mg-porphine molecule. The Mg-N, N-C, C-C, and C-H bond lengths are 2.08, 1.38, 1.40–1.45, and 1.09 Å, respectively. The calculated energy levels and the wave functions of key states of the neutral Mg-porphine molecule are presented in blue color in Fig. 1. The wave function of its LUMO state consists of eight major lobes in the C-pentagons, in good accordance with the STM images. The LUMO+1 state is more symmetric, with the C-C π-bonding feature. Note that the wave functions of LUMO and LUMO+1 have nodes at the Mg site and hence the STM tunneling current is zero at the center of molecule in the ideal case. To investigate correlation effects, we also studied the charged state of the molecule, produced when an extra electron is added. Significantly, we found through DMol calculations that the $-e$ charged state is more stable than the neutral state with an energy gain as large as 1.30 eV. This energy corresponds to the strength of Coulomb correlation U for the LUMO state. The experimental value of U in Ref. 4 deduced from the dI/dV curve is 1.15 eV, in excellent agreement with our calculations. In the charged state, the Mg-porphine molecule possesses a magnetic moment of $1.0\mu_B$. Charge partitioning by the Hirshfeld method and Mulliken population analysis indicate that the magnetization mainly occurs on the C sites whereas the magnetic moments of N and Mg are much smaller (by an order of magnitude). As a result, we find that the LUMO state splits to LUMO-α (or spin up) and LUMO-β (or spin down) states, very much as found experimentally by Wu, Ogawa, and Ho.[4] Our calculated energy for the LUMO+1 state also nicely matches the peak position in the dI/dV curve. We thus see that the DFT calculations for the isolated molecule capture all the main features of experimental data measured on the alumina/NiAl(110) substrate.

B. Effect of substrate: Influence of electric-field fluctuations

To calculate the matrix elements which appear in the expression for the proper self-energy, we have used real-space integration based on the wave function obtained through the VASP calculations. To appreciate the range of wave vectors which are significant in the integration over the variable $Q_{\parallel}$, in Fig. 2 we show the matrix element $M_{\alpha\alpha}(\vec{Q}_{\parallel}) = |\langle\alpha|\exp(i\vec{Q}_{\parallel}\cdot\vec{r}_{\parallel} - Q_{\parallel}z|\alpha\rangle|^2$ for the case where the state $|\alpha\rangle$ is the LUMO orbital. The striking point is that this matrix element drops to nearly zero by the time $Q_{\parallel}$ is the order of 10^7 cm^{-1}. This is a consequence of the fact that the Mg-porphine molecule is rather large. We may expect, by virtue of the factor of $\exp(i\vec{Q}_{\parallel}\cdot\vec{r}_{\parallel})$ in the matrix element, that the matrix element falls off rapidly when $|\vec{Q}_{\parallel}|$ becomes larger than the inverse linear dimensions of the imprint of the molecule on the xy plane, and we see from Fig. 2 that this is indeed the case. The matrix elements such as $M_{\alpha\alpha}(\vec{Q}_{\parallel})$ depend on the direction of $\vec{Q}_{\parallel}$ as well as its magnitude. We find, however, that virtually all of the matrix elements show only a very modest dependence on the direction of $\vec{Q}_{\parallel}$. Thus when we evaluated the various contributions to the proper self-energy, we assumed all matrix elements are functions simply of the magnitude of $\vec{Q}_{\parallel}$.

The fact that the matrix elements fall off so rapidly with the magnitude of $\vec{Q}_{\parallel}$ ensures that our description of the electric-field fluctuations through use of the continuum approximation for the description of the substrate should be quite adequate from the quantitative point of view, it should be noted.

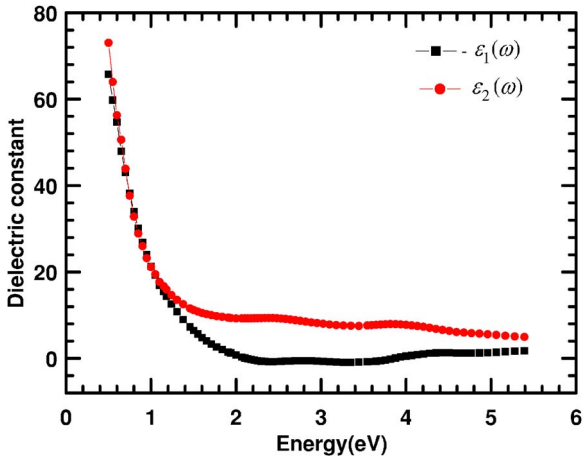

FIG. 3. (Color online) The real and imaginary parts of the dielectric constant of NiAl in the range 0.5 to 5.5 eV. The data have been provided by Joo Yull Rhee. Notice that it is the negative of $\varepsilon_1(\omega)$ that is plotted in the graph.

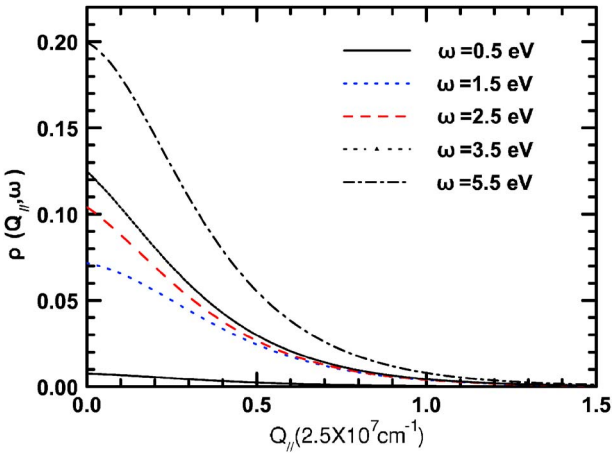

FIG. 4. (Color online) We show the wave-vector dependence of the function $\rho(Q_\parallel,\omega)=\mathrm{Im}\{-1/[\tilde{\varepsilon}(Q_\parallel,\omega)+1]\}$ for several frequencies.

To complete the calculation of the proper self-energy, of course we also need the function $\rho(\vec{Q}_\parallel,\omega)=\mathrm{Im}\{-1/[\tilde{\varepsilon}(Q_\parallel,\omega)+1]\}$. In our calculations, we have taken the dielectric constant of the oxide layer to be real, independent of frequency, and equal to the value 4. Our final results are not sensitive to the precise value of the dielectric constant of the oxide layer. The primary role of the oxide is, as stressed in Sec. I, to decouple the orbitals of the molecular adsorbate from those of the electrons which reside in the substrate.

Of course, we require the real and the imaginary part of the frequency-dependent dielectric constant of the NiAl substrate. While we have found various papers which provide us with the frequency dependence of the real part of the optical conductivity of this material, from which the imaginary part of the dielectric constant may be constructed, we are unaware of any papers in the literature which present us with both the real and the imaginary part of the frequency-dependent dielectric constant. Even data on the real part of the optical conductivity does not extend over a wide enough frequency range to allow construction of its imaginary part via a Kramers-Kronig transform. We have been informed[15] that Joo Yull Rhee has measured both the real and imaginary part of the optical dielectric constant of NiAl, and he has kindly provided us with his data, which extend from 0.5 to 5.5 eV.[16] The data are reproduced in Fig. 3. Notice that the black curve is the negative of $\varepsilon_1(\omega)$.

Upon examining the data in Fig. 3, it is evident that throughout the optical frequency range, the imaginary part of the dielectric constant is very substantial in magnitude. It appears that this surface does not support surface plasmons in the frequency range displayed. For this, the condition $\varepsilon_1(\omega)=-1$ must be satisfied, and in this spectral range the imaginary part should be small if the surface plasmons are to exist as long-lived, well-defined excitations. The large imaginary part will also make the function $\rho(Q_\parallel,\omega)$ rather modest in value. Thus we can expect that the contribution of the electric-field fluctuations to the real part of $\delta\Sigma_{\alpha\alpha}$ defined in Eq. (34b) will be rather small, and we shall see that this is indeed the case.

In Fig. 4, we show the wave-vector dependence of $\rho(Q_\parallel,\omega)$ for several frequencies of interest. We see that once again the important wave vectors lie in the range of 10^7 cm^{-1} or below. This further reinforces the point that our long-wavelength description of the electromagnetic fluctuations is quite adequate for our purposes here, for quantitative calculations.

In Table I, we summarize our calculations of the real part of the proper self-energy, for the highest occupied molecular orbital (HOMO) orbital, the two (nondegenerate) LUMO orbitals, and also the LUMO+1 state. As remarked above, the real part of the self-energy describes the change in excitation energy associated with a given state. Thus the negative signs in the LUMO states and the LUMO+1 mean that the energy level of the orbital is shifted downward, so the excitation energy to promote an electron from the Fermi energy has decreased. Since the HOMO is occupied, an upward shift of the orbital decreases the excitation energy of this state, which involves hole creation. Thus all orbitals are shifted downward by the energy correction described by the proper self-energy.

In the sums over excited states, all states within ±20 eV of the energy of the HOMO orbital were included. The real part of the self-energy is dominated by the diagonal part given in Eq. (33), and for this system the contribution from virtual fluctuations into excited states is rather small. We hasten to remark that to calculate this contribution accurately, unfortunately we need optical data that extend well beyond 5.5 eV. One may appreciate this from Fig. 4, where

TABLE I. The real part of the self-energy for the four orbitals indicated.

Orbital	$\Sigma^{(D)}_{\alpha\alpha}$ (meV)	$\delta\Sigma_{\alpha\alpha}$ (meV)
HOMO	65.73	1.201
LUMO^1	−64.24	−1.557
LUMO^2	−66.01	−1.490
LUMO+1	−63.96	−5.000

one sees that the largest contribution to the energy shift comes from the upper end of the data displayed in Fig. 3. Thus our calculations may underestimate the contribution from the virtual fluctuations by a considerable amount. It is, unfortunately, rather difficult to develop an extrapolation of the dielectric constant data to higher frequencies from the data in hand. However, even if the errors introduced by the 5.5-eV upper cutoff in the frequency integration were substantial, it would seem that for the system explored here, the contribution to the real part of the self-energy from virtual fluctuations would remain a modest contribution in the end. It is not clear to us that this will be the case for other adsorbate or substrate contributions, particularly when the substrate supports surface plasmons in the frequency range where the fluctuation induced virtual transitions to excited states can occur. One can envision near resonant coupling between the molecule and the surface plasmons when this happens.

In our picture, if we set the small splitting between the two LUMO states aside, then the lifetime of both the LUMO complex and the HOMO state is infinite. Of course, hybridization between these orbitals and the conduction electron states of the substrate, not considered here, will result in a finite nonradiative lifetime for these states. There must be empty, unoccupied states below an excited state for the electron to fall into in order for the state to acquire a finite nonradiative lifetime within the picture set forth here. Thus we do find a finite nonradiative decay rate for the LUMO+1 state probed in Ref. 4. For this state, the imaginary part of the proper self-energy is 6.62 meV. The nonradiative lifetime $\tau=\hbar/\mathrm{Im}\{\Sigma_{\alpha\alpha}\}$ of the LUMO+1 state would then be very close to 0.1 ps. In the final section of the paper, we shall discuss some implications of the results given above.

IV. GENERAL DISCUSSION AND CONCLUDING REMARKS

We have developed the theory of the interaction of adsorbate molecules and atoms with electric-field fluctuations necessarily present above any substrate on which the molecule is adsorbed. The field fluctuations have their origin in the thermodynamic fluctuations in charge density necessarily present within the substrate, and electrons within the molecule sense these fluctuations through the long-ranged tail of the Coulomb interaction. These fluctuations lead to energy shifts of the various atomic or molecular orbitals not included in standard density-functional treatments of such systems, and in addition to those excited states higher in energy than the LUMO acquire a finite lifetime by virtue of nonradiative transitions to lower energy unoccupied states. The description set forth here is particularly useful for the discussion of entities adsorbed on oxide covered surfaces, since in the presence of the oxide barrier direct hybridization between the adsorbate and substrate orbitals can be overlooked to first approximation. We do expect that for species strongly chemisorbed on metal surfaces, the strong hybridization necessarily present will dominate the fluctuation effects studied here, though it remains the case that the interactions studied here will also be present.

We have applied the theory to the calculation of the energy shift of the HOMO orbital, the LUMO orbitals, and the LUMO+1 orbital, for the Mg-porphine molecule adsorbed on the oxide covered NiAl(110) surface. This is the system studied in detail in Ref. 4. The level shifts are in the range of 65 meV for all these states, and the dynamical contribution to this effective image potential shift is a small fraction of the total. As noted in Sec. III, this will not necessarily be the case in other systems, in our view.

To make contact with the data of Ref. 4, it will be necessary to take into account the influence of the STM tip, which is physically large (200-Å radius of curvature, typically) and as close to the molecule as the substrate itself. The formalism here, in combination with the developments described in Ref. 11, will allow this extension to be made. We may employ the same orbitals developed for the present study, and the mathematical formalism developed in Ref. 11 will allow the incorporation of the influence of the STM tip on the electric-field fluctuations near the molecule. If the STM tip is made from, say, Ag, the results described in Ref. 11 lead us to expect that the influence of the tip may be significant.

We have seen that the width with origin in nonradiative decay of the LUMO+1 state is in the range of 6.6 meV. We have been informed that the width of the LUMO+1 state has been inferred experimentally.[17] The results vary from 2 to 10 meV for various molecules probed. Our calculated width lies in the middle of this range, and we thus regard the agreement between theory and experiment as quite satisfactory.

It was found in Ref. 4 that the negatively charge state of the Mg porphine molecule is stable, a result that follows also from our density-functional studies reported in Sec. III A above. In the experiments of Ref. 4, to form the negatively charged state, the electron is injected into the LUMO+1 orbital. This electron will then decay to the LUMO manifold in roughly 0.1 ps according to the calculation presented here, through transfer of energy to the particle-hole pairs of the NiAl substrate. This time is short compared to the radiative lifetime of the LUMO+1 state, as we will see below. The electron is then trapped in a long-lived LUMO state, and the lifetime of the LUMO state is evidently long enough for the nuclei in the molecule to relax, thus driving the LUMO state below the Fermi level, to form the new level observed in Ref. 4 and found also in our density-functional study. The stability of the negative ion state, in our view, is a consequence of the long lifetime of the LUMO state, when the molecule sits on the oxide barrier.

It is highly desirable to detect photons radiated by molecules such as that studied in this paper, so one can do single molecule spectroscopy on such entities. The STM can inject electrons into excited states, possibly in a photon assisted manner as in Ref. 4, and by detecting radiated photons one can gain information regarding the electronic structure of the adsorbate. In this regard, the quantum efficiency of the radiation process is of great interest. To estimate this, we need the probability that the molecule, with an electron in its excited state, will emit a photon. For the Mg-porphine molecule discussed above, a crude estimate of the quantum efficiency may be obtained by simply calculating the transition rate for transitions from the LUMO+1 to the LUMO state

with the molecule in free space, and then we may compare with the nonradiative transition rate discussed above. It turns out that this transition is dipole allowed, and the transition dipole moment is parallel to the surface. We have calculated the dipole matrix element to find $|\langle \mathrm{LUMO}+1|p_x|\mathrm{LUMO}\rangle|^2 = |\langle \mathrm{LUMO}+1|p_y|\mathrm{LUMO}\rangle|^2 = 3.79\times 10^{-20}$ cgs units while the matrix element of p_z vanishes. If this is inserted into the Fermi Golden Rule for dipole transition rates for an entity in free space, we find the free-space radiative lifetime to be 53 ns. This suggests that the quantum efficiency is very small, in the range of 2×10^{-6}. This estimate does not take due account of the influence of the substrate on the radiation rate, and for a parallel dipole the estimate just given should be regarded as an upper bound on the radiative rate.

It is the case in the experiments reported in Ref. 4 that the photon emission rate was found to be substantially enhanced when a Ag-coated tip was employed rather than a W tip. This suggests that surface plasmon enhancements of the sort discussed in Ref. 11 are present, by virtue of the Ag tip. Further comments on this issue await incorporation of the role of the STM tip on the electric-field fluctuations near the molecule.

ACKNOWLEDGMENTS

We are grateful to Wilson Ho and Shiwei Wu for discussions of this research. Also, we appreciate interactions with D. W. Lynch concerning the optical properties of NiAl, and we are especially grateful to Joo Yull Rhee for kindly providing us with his data on the optical dielectric constant of NiAl. This research has been supported by the Office of Basic Energy Sciences of the U. S. Department of Energy. The research of D.L.M. was supported by Grant No. DE-FG03-84ER-45083, and that of J.X.C. and R.W. was supported by Grant No. DE-FG02-04ER-15611. The calculations reported here were conducted on supercomputers at NERSC.

[1] B. C. Stipe, M. A. Rezai, and W. Ho, Science **280**, 1263 (1998).
[2] L. J. Lauhon and W. Ho, Phys. Rev. Lett. **85**, 4566 (2000).
[3] Examples of the use of STM spectroscopy to study electronic levels are found in H. J. Lee, W. Ho, and M. Persson, Phys. Rev. Lett. **92**, 186802 (2004); T. M. Wallis, N. Nilius, and W. Ho, J. Chem. Phys. **119**, 2296 (2003). A comparison between spectra taken for C_{60} molecules adsorbed directly on NiAl(110) and the same surface with an oxide layer is given by N. A. Pradhan, N. Liu, and W. Ho, J. Phys. Chem. B **109**, 8513 (2005).
[4] S. W. Wu, N. Ogawa, and W. Ho, Science **312**, 1362 (2006).
[5] See the discussion in *Methods of Quantum Field Theory in Statistical Physics*, edited by A. A. Abrikosov, L. P. Gor'kov, and I. E. Dyaloshinskii (Prentice-Hall, Inc., Englewood Cliffs, NJ, 1963), Chap. 6.
[6] D. L. Mills, Surf. Sci. **48**, 59 (1975).
[7] See the discussion in *Electron Energy Loss Spectroscopy and Surface Vibrations*, edited by H. Ibach and D. L. Mills (Academic Press, San Francisco, 1982), Chap. 3.
[8] L. H. Dubois, G. P. Schwartz, R. E. Camley, and D. L. Mills, Phys. Rev. B **29**, 3208 (1984).
[9] D. L. Mills, R. B. Phelps, and L. L. Kesmodel, Phys. Rev. B **50**, 6394 (1994).
[10] For a discussion of the inclusion of the image potential effects, see M. Heinrichsmeier, A. Fleszar, W. Hanke, and A. G. Eguiluz, Phys. Rev. B **57**, 14974 (1998), and recently a formal means of incorporating the van der Waals potential has appeared, with application to small systems. See M. Dion, H. Rydberg, E. Schroder, D. C. Langreth, and B. I. Lundqvist, Phys. Rev. Lett. **92**, 246401 (2004).
[11] D. L. Mills, Phys. Rev. B **65**, 125419 (2002); Shiwei Wu and D. L. Mills, *ibid.* **65**, 205420 (2002).
[12] See D. L. Mills, Phys. Rev. B **62**, 11197 (2000), Eq. (2.35).
[13] B. Delley, J. Chem. Phys. **92**, 508 (1990); **113**, 7756 (2000).
[14] B. Hammer, L. B. Hansen, and J. K. Norskov, Phys. Rev. B **59**, 7413 (1999).
[15] D. W. Lynch (private communication). We are grateful to D. W. Lynch for discussions of optical measurements of the properties of NiAl.
[16] Joo Yull Rhee (private communication). For a discussion of the real part of the optical conductivity of FeAl, NiAl, and CoAl and comparison between experiment and theory, see J. Y. Rhee, J. Korean Phys. Soc. **43**, 1091 (2003).
[17] Shiwei Wu and Wilson Ho (private communication).